Journal of Earthquake and Tsunami
(2024)

DOI: 10.1142/S179343112450026X

Life-Cycle Cost Assessment of the Base-Isolated-Reinforced Concrete Structure

Hao Wang [*,‡], Xiaoxia Guo [†,§], Chao Luo [*,¶], Jun Zhao [†,‖] and Huaiping Feng [*,**]

[*]*State Key Laboratory of Mechanical, Behavior and System Safety of Traffic, Engineering Structures, Shijiazhuang Tiedao University, Shijiazhuang, P. R. China*

[†]*School of Civil Engineering, Shijiazhuang Tiedao University, Shijiazhuang, P. R. China*

[‡]*wanghao@stdu.edu.cn*

[§]*12021011167@student.stdu.edu.cn*

[¶]*luochao@stdu.edu.cn*

[‖]*12022201307@student.stdu.edu.cn*

[**]*fenghuaiping@stdu.edu.cn*

Received 28 January 2024
Revised 11 July 2024
Accepted 24 July 2024
Published 19 September 2024

Seismic isolation structures have excellent seismic mitigation effects, but implementing isolation measures may increase the initial cost of the structure. This paper presents a method to calculate the seismic loss and assess the life-cycle cost of isolated structures, which is convenient for owners to make decisions. The life-cycle cost assessment model is divided into two parts: initial cost assessment and seismic loss assessment over life-cycle period. Among them, the assessment method of the isolation layer is proposed, including the cost assessment of isolation bearings and dampers. The assessment method of seismic loss considers direct loss, indirect loss, casualties and integrating casualties into a unified assessment system. Direct loss includes building loss, indirect loss includes rental loss, relocation loss, income loss, personal property loss and business inventory loss. The seismic loss model is associated with seismic damage probability, which is obtained through seismic vulnerability and seismic probability risk assessment. The 8-story base-isolated-reinforced concrete structure illustrates the feasibility of the life-cycle-cost assessment model. The example shows that the initial cost of the isolated structure exceeds that of the nonisolated structure, however, the rental loss, income loss, personal property loss and casualties are much lower than those of nonisolated structures. The income loss of the isolated structure is the maximum proportion in life-cycle cost, and the casualty loss is the minimum proportion in the seismic loss, due to its excellent seismic mitigation effects.

Keywords: Life-cycle cost assessment; seismic isolation structure; seismic loss; seismic risk assessment; casualties.

[¶]Corresponding author.

1. Introduction

With the continuing development of the social economy and the steady increase in population density, the occurrence of a major earthquake carries the potential for significant economic losses and profound social consequences. In 2011, a devastating 9.0 magnitude earthquake struck Japan, as documented by Norio *et al.* [2011]. This catastrophic event resulted in the tragic loss of 13,392 lives, with an additional 15,133 people reported as missing. The economic impact was staggering, reaching an estimated range of 171–183 billion USD in losses. The 2017 earthquake in Mexico [Galvis *et al.*, 2020] resulted in tragic casualties and injuries to 369 people. It also caused significant damage, collapsing 44 buildings and 2 bridges. Nowadays, base-isolated has become a well-established engineering technology for mitigating the effects of seismic events [Wang *et al.*, 2021; Sevim *et al.*, 2024; Katsamakas *et al.*, 2021]. The effectiveness of smart base-isolation is studied by using a smart base-isolation system in LNG, the results show that a smart base-isolation system can effectively reduce the seismic response of very large LNG storage tanks [Kharde and Soni, 2022]. Seismically isolated structures are designed to maintain structural integrity and ensure the safety of internal building facilities, effectively reducing the casualty and economic damage caused by earthquakes. However, it is important to note that the implementation of seismic isolation technology involves an initial increase in construction costs. Assessing whether the additional investment is worthwhile for the owner is a complex task, as it involves evaluating various factors and long-term outcomes. The damage and collapse of buildings caused by earthquakes and tsunamis are studied, and the types and causes of damage occurring on RC and masonry structures are assessed [Altunişik *et al.*, 2021]. This paper summarizes the common structural deformations and failures of RC, and evaluates the performance of existing buildings based on field observations. The results show that the existing buildings in Japan are not sufficiently resistant to earthquakes. It is suggested to strengthen the existing structures and provide appropriate schemes for the design of new buildings [Altunişik *et al.*, 2023]. The performance-based seismic design method by Demir *et al.* [2021] provides a valuable approach to assessing structural performance, offering the flexibility to select performance indicators tailored to the owner's requirements [Gil Oulbé *et al.*, 2020]. This method allows for a more personalized and targeted assessment, ensuring that the design meets the specific needs and priorities of the owner. By using life-cycle cost as a control performance indicator for the design of base-isolated structures, it becomes possible to minimize structural damage and losses while optimizing cost efficiency. This approach ensures that the designed structure achieves a balance between mitigating seismic risks and minimizing long-term expenses. While some scholars have incorporated the performance-based seismic design framework into the seismic design of isolated structures, the exploration of life-cycle cost as an indicator remains relatively limited. Liu *et al.* [2023] believed that establishing a life cycle assessment model to estimate costs and cash flows at each stage is an effective approach. The results indicate that this method can provide

accurate and reliable recommendations for wind power economic assessment in various regions and environments, offering valuable reference for enhancing the economic benefits of wind farms. Calculating both direct and indirect losses based on previous data lacks sufficient theoretical models and poses challenges for widespread application. Lee *et al.* [2023] proposed that engineering classification codes can serve as computational tools for estimating the initial cost of structures, thereby indirectly providing calculations for the life-cycle cost. Arash Rayegani [2022] utilized the exceedance probability of each damage state to assess the direct and indirect damage costs of seismic isolation structures. The results indicate that seismic isolation systems can effectively reduce the cost of losses. Nouri *et al.* [2022] conducted a study exploring the assessment of life-cycle costs in reinforced concrete structures, considering various aspects including construction, social and environmental factors. Their research delves into a comprehensive analysis, providing valuable insights into the holistic assessment of life-cycle costs associated with reinforced concrete structures. Structural losses include the initial cost of the structure, while social losses include factors such as repair costs, material destruction costs, rental costs, income loss, injury costs and casualty. Additionally, environmental loss includes the cost associated with carbon emissions, PM2.5 particle pollution, fossil fuel resource depletion and water consumption. This comprehensive approach allows for a more thorough assessment of the life-cycle costs considering multiple dimensions. To facilitate comparative analysis, each of these costs was converted into net present value, which takes into account the annual inflation rate and seismic damage probability. This conversion allows for a more accurate assessment of the long-term financial implications and seismic risks associated with the evaluated costs. Du *et al.* [2021] conducted nonlinear seismic response analyses on both isolated and non-isolated-reinforced concrete structures. Their objective was to evaluate structural performance parameters under different levels of seismic hazard. By analyzing the response of these structures, valuable insights were gained into their performance and behavior in the face of different seismic hazards. The seismic performance of structures can be quantified through various measures, including the frequency of repairs, the associated repair costs and the assessment of casualties. These quantifiable factors provide valuable indicators for evaluating the resilience and effectiveness of structures in withstanding seismic events. An intensity-based assessment methodology was used to compare and analyze each performance measure. This method provided a comprehensive assessment of the structural response and behavior under different intensities of seismic events. The comparison and analysis of the results provided valuable insights for the design and optimization of structures for improved seismic performance. However, it should be noted that the modeling of collapse vulnerability and loss for isolated structures was not included in the analysis. In addition, the study did not consider the additional costs and maintenance time associated with nonstructural components. These aspects represent important considerations that should be addressed in future research to provide a more comprehensive understanding of the overall performance and cost implications of isolated

structures. Furthermore, it is important to acknowledge that the results of the study were limited to a single specific case study. In related research, Aykanat *et al.* [2023] conducted on-site seismic damage investigations in the Golyaka district to thoroughly assess the types and causes of damage to reinforced concrete and masonry structures. They also evaluated the seismic hazard of the area by considering the casualties and property losses caused by earthquakes over the years. This research contributes valuable insights to the field, but it is essential to conduct further studies and case-specific analyses to broaden our understanding of the performance and cost implications of such isolation systems in different scenarios. Dolce *et al.* [2021] put forth a seismic risk assessment method specifically tailored for residential buildings. Their research introduced calculation methods for quantifying various earthquake-related impacts, including casualty, direct losses, unusable buildings and displacement of residents. Additionally, they made significant contributions by updating the seismic risk map of residential buildings in Italy. These advancements provide valuable tools and insights for assessing and mitigating seismic risks in residential areas. Through the aforementioned literature review, it becomes evident that there is a current deficiency in having a comprehensive assessment model for assessing seismic loss and conducting life-cycle cost analysis specifically tailored for base-isolated buildings. Further research and development are needed to address this gap and provide a standardized framework that enables accurate and holistic assessments of seismic risks, losses and cost implications for base-isolated structures.

The purpose of this paper is to develop a performance-based seismic loss assessment method and life-cycle cost assessment method for base-isolated structures. The life-cycle cost assessment model consists of two parts, including initial cost and seismic loss. Firstly, the initial cost assessment model is proposed, the initial cost of the isolation layer including the initial cost of isolation bearings and dampers. Secondly, the seismic loss model is associated with seismic vulnerability and seismic probability risk assessment. Direct loss includes building loss, indirect loss includes rental loss, relocation loss, income loss, personal property loss, business inventory loss and casualty. In addition, this paper quantifies the cost of casualties to integrate casualties into a unified assessment system. Finally, the life-cycle cost is proposed to be the sum of the seismic loss and the initial cost. The application of an 8-story base-isolated-reinforced concrete structure illustrates the feasibility of the life-cycle-cost assessment method. The proportion of initial cost and building loss, rental loss, relocation loss, income loss, personal property loss, business inventory loss and casualty of the isolated and nonisolated structures is studied, and the seismic loss and life-cycle cost of isolated and nonisolated structures are compared.

2. Life-Cycle Cost Assessment Framework

Life-cycle cost refers to all the costs incurred throughout the life of a building, from its construction to the time of demolition. The life-cycle cost assessment in this paper is an overall assessment of the initial cost, maintenance and demolition costs during

the building's lifespan, and the losses due to seismic failures. This assessment provides a quantitative understanding of the extent of structural seismic damage, which allows for informed decision-making in construction [O'Reilly and Calvi, 2019]. The costs associated with the maintenance and demolition of structures can be considered as a form of seismic loss. Therefore, it is possible to combine and integrate the costs related to structural maintenance, demolition and seismic failure losses into a unified consideration. The life-cycle cost assessment of a building structure can be evaluated using a model that takes into account the discount rate. It can be represented as Eq. (1).

$$E[C_{\mathrm{LCC}}] = C_I + \frac{(1 - e^{-\lambda t})}{\lambda} \mathrm{DV}, \tag{1}$$

where C_{LCC} is the total life cycle of the structure; $E[C_{\mathrm{LCC}}]$ is the expected life-cycle cost; C_I is the initial cost of the structure; DV is the decision variable for seismic risk and can be represented by seismic losses; $e^{-\lambda t}$ is the discount factor, where λ is the annual discount rate. FEMA P-58-1 Agency [2018] recommends an annual discount rate of 3%–4% for public buildings and 4%–6% for nonpublic buildings; t is the structural lifespan.

To more accurately assess the costs associated with structural seismic damage, the structural damage state is divided into several levels. The probability of each damage level occurring during the life of the structure is calculated, and the required repair cost and repair time for each seismic damage state level are evaluated accordingly. Thus, the life-cycle cost of a structure can be expressed by Eq. (2).

$$E[C_{\mathrm{LCC}}] = C_I + \frac{(1 - e^{-\lambda t})}{\lambda} \sum_{i=1}^{n} \mathrm{DV}_i, \tag{2}$$

where DV_i are the seismic losses caused by structural damage occurring at the ith level of failure.

As can be seen from Eq. (2), the key to evaluating the life-cycle cost of structures in performance-based seismic design is to estimate the losses due to structural damage caused by earthquakes. In this paper, the life cycle cost assessment is divided into two main steps. The first step involves the evaluation of seismic damage probabilities throughout the structural lifetime using a performance-based probabilistic seismic risk assessment framework. The performance-based probability seismic risk assessment framework expresses the structural damage probability in the form of "seismic risk × seismic vulnerability" as Eq. (3).

$$\lambda_{\mathrm{DV}}(\mathrm{dv}) = \int_{\mathrm{im}} G(\mathrm{dm}|\mathrm{im}) |d\lambda_{\mathrm{IM}}(\mathrm{im}), \tag{3}$$

where $\lambda_{\mathrm{DV}}(\mathrm{dv}) = P(\mathrm{DV} \geq \mathrm{dv})$ is the probabilistic seismic risk, $(\mathrm{DV} \geq \mathrm{dv})$ denotes the annual probability of the occurrence; $G(x|y) = P(X \geq x|Y = y)$ is the cumulative distribution function of a random variable X conditioned on $Y = y$;$G(\mathrm{dm}|\mathrm{im}) = P(\mathrm{DM} \geq \mathrm{dm})$ is the seismic vulnerability function, which

represents the probability of exceeding a certain damage threshold for a given seismic ground motion intensity; and $\lambda_{\mathrm{IM}}(\mathrm{im}) = P(\mathrm{IM} \geq \mathrm{im})$ is the site hazard model, which characterizes the annual exceedance probability of a certain seismic ground motion intensity at a specific site.

From Eq. (3), it can be inferred that by integrating seismic vulnerability analysis, seismic hazard analysis and probabilistic seismic risk analysis, the probability of structural damage under earthquake loading can be obtained. Let y be the structural response, and LS_i be the ith state limit. The damage probability at various performance levels can be calculated using Eq. (3) as given by Eqs. (4) and (5).

$$P_{\mathrm{LS}_i} = P[y \geq \mathrm{LS}_1]. \tag{4}$$

$$P_{\mathrm{DS}_j} = P[\mathrm{LS}_{i-1} \leq y \leq \mathrm{LS}_i], \tag{5}$$

where P_{LS_i} is the probability of the structural performance state exceeding ith is the limit state; and P_{DS_j} is the probability of the structural performance state at jth damage state.

Assuming that the structural performance state is divided into five levels, the relationship between the probability of the structure exceeding a given limit state and the probabilities of the structure being in different damage states can be expressed by Eq. (6), as shown in Fig. 1.

$$P_{\mathrm{LS}_i} = \sum_{j=i+1}^{5} P_{\mathrm{DS}_i}. \tag{6}$$

The second step involves evaluating the seismic losses caused by structural earthquake damage and integrating it with the initial cost of the structure to assess the life-cycle cost. In this step, the seismic damage state of the structure is related to the seismic losses, repair time and repair cost of the structure. According to the total probability theory, the total seismic failure losses of the structure can be expressed as Eq. (7).

$$\mathrm{DV} = \sum_{j=1}^{n} P_{\mathrm{DS}_j} \mathrm{DV}_j. \tag{7}$$

Flowchart of the life-cycle cost assessment is shown in Fig. 2.

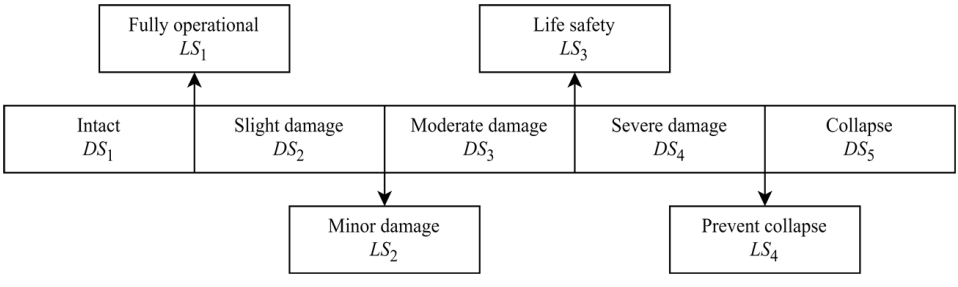

Fig. 1. The relationship between the four performance levels and the five damage states diagram.

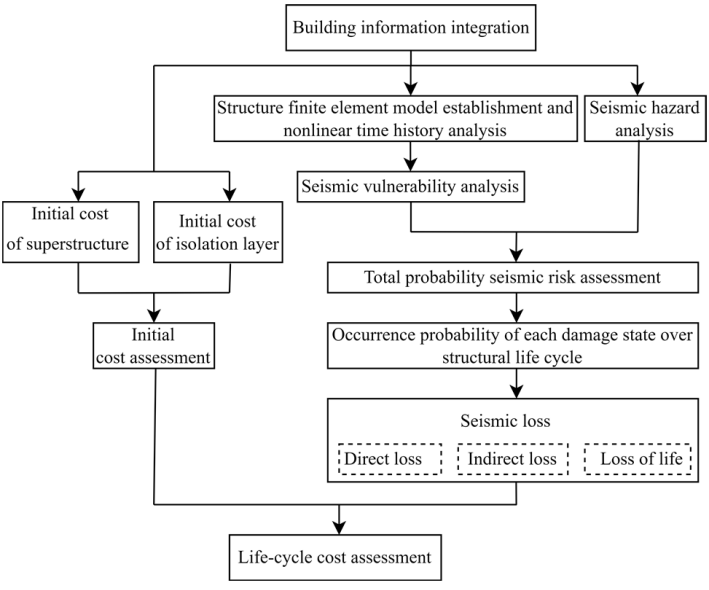

Fig. 2. Flowchart of the life-cycle cost assessment.

2.1. *Assessment of structural seismic damage probability*

From Eq. (3), it can be inferred that the assessment of structural damage probability can be divided into three aspects: seismic vulnerability analysis, seismic hazard analysis and seismic probabilistic risk analysis.

Step I: Seismic vulnerability analysis based on response surface method. To reduce the computational cost of seismic vulnerability analysis, this study introduces the response surface method to calculate the seismic vulnerability of structures. The basic idea of the response surface method is to approximate the actual structural performance function with a simple explicit function.

The dual response surface method involves collecting samples repeatedly during each run of the experimental design. The mean of the samples is used as one response input, while the standard deviation of the samples is used as the second response input. The mean response is used to achieve the desired fit, while the standard deviation of the response ensures the robustness of the fit function against uncontrollable factors. The mean and standard deviations of the response surface function using ground motion intensity as an input parameter are

$$\hat{y}_\mu = g(\mathbf{x}, \mathrm{IM}), \tag{8}$$

$$\hat{y}_\sigma = h(\mathbf{x}, \mathrm{IM}). \tag{9}$$

Assuming that the structural response follows a normal distribution, the response surface function can be expressed as

$$\hat{y} = g(\mathbf{x}, \mathrm{IM}) + N[0, h(\mathbf{x}, \mathrm{IM})]. \tag{10}$$

Using a quadratic polynomial to represent the response surface function offers the advantages of reduced computational complexity, improved computational stability and higher accuracy [Li and Yang, 2019]. Quadratic polynomial is used as the structural response function

$$\hat{Z} = \hat{g}(\mathbf{X}) = a + \sum_{i=1}^{n} b_i X_i + \sum_{i=1}^{n} c_i X_i^2, \tag{11}$$

where a, b_i and c_i are the coefficients to be determined for the expressions.

Perform regression fitting on the response surface function. According to the combined samples of input and output variables obtained from the experimental design, the undetermined coefficients a, b_i and c_i in Eq. (11) can be obtained by least squares fitting.

A flowchart of seismic vulnerability analysis based on the dual response surface method is shown in Fig. 3.

The probability of exceeding a certain damage limit for a structure at a given seismic intensity is obtained through vulnerability analysis.

The failure of any component within the superstructure or isolation layer will fail the entire base-isolated structure. Therefore, the superstructure and isolation layer can be regarded as a "series" system. If any response of MSD (maximum superstructure displacement) or MDIL (maximum displacement of isolation layer) exceeds its limit state, the seismic isolation system is considered to have failed at a specific limit state [Wang and Huang, 2021]. Assuming MSD and MDIL are statistically

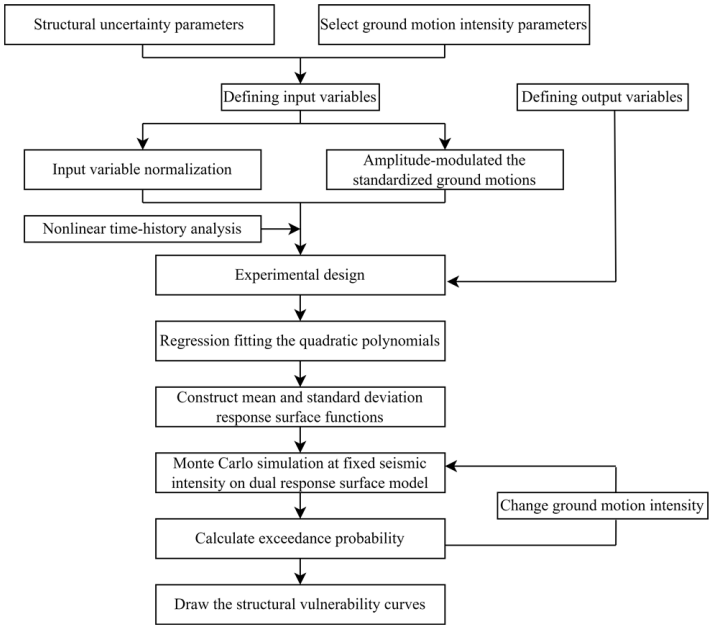

Fig. 3. Flowchart of vulnerability analysis based on dual response surface method.

independent, the overall probability of exceeding the seismic isolation structural system can be approximated using Eq. (12).

$$P(F_{\text{system}}) = 1 - \prod_{i=1}^{m} [1 - P(F_i)], \tag{12}$$

where $P[F_i]$ is the failure probability of the substructure exceeding ith limit state, and $P[F_{\text{system}}]$ is the failure probability of the overall structure exceeding ith limit state.

Step II: Seismic hazard analysis. Seismic hazard refers to the magnitude and frequency of seismic effects that a particular site may experience over a certain period. The Gerstenberger *et al.* [2020] seismic hazard probability model is the annual exceedance probability of a certain ground motion intensity at a specific site.

Cornell [1968] demonstrated that there is a logarithmic-linear relationship between the annual maximum ground acceleration or spectral acceleration and the probability of exceeding a certain threshold of acceleration for moderate to major earthquakes [Astorga *et al.*, 2020]. The seismic hazard probability model can be described using the maximum value distribution function of the extreme type 2, as shown in Eq. (13).

$$\lambda_{\text{IM}}(\text{im}) = P[\text{IM} \geq x] = 1 - \exp\left[-\left(\frac{x}{u}\right)^{-k}\right], \tag{13}$$

where u is the seismic magnitude parameter, and k is the shape parameter of the seismic hazard curve.

The power-law exponent is used to approximate the log-linear relationship

$$\nu_{\text{IM}}(\text{im}) = \left(\frac{\text{im}}{u}\right)^{-k} \approx k_0 \cdot (\text{im})^{-k}, \tag{14}$$

where $v_{\text{IM}}(\text{im})$ is the annual average exceeding the probability of the ground motion intensity parameter, k_0 are the shape factors of the seismic hazard curve. k and k_0 can be determined by two-point interpolation of the annual average frequency of $1/475$ (50-year exceeding probability 10%) and the annual average frequency of $1/2475$ (50-year exceeding probability 2%) [Bashir and Basu, 2018].

$$k = \frac{\ln(\nu_{10\%}/\nu_{2\%})}{\ln(\text{Sa}_{2\%}/\text{Sa}_{10\%})}. \tag{15}$$

$$\ln(k_0) = \frac{\ln(\text{Sa}_{10\%}) \cdot \ln(\nu_{2\%}) - \ln(\text{Sa}_{2\%}) \cdot \ln(\nu_{10\%})}{\ln(\text{Sa}_{10\%}/\text{Sa}_{2\%})}, \tag{16}$$

where $\text{Sa}_{10\%}$ and $\text{Sa}_{2\%}$ are the ground motion spectrum acceleration corresponding to the 50-year exceeding probability of 10% and 2%, respectively; $v_{10\%}$ and $v_{2\%}$ are the annual exceedance probability $1/475 = 0.0021$, $1/2475 = 4.04 \times 10^{-4}$, respectively.

Step III: Seismic probabilistic risk assessment. Seismic risk assessment refers to assessing the degree of damage to buildings and the loss to society caused by earthquakes within a specified time.

The annual probability of structural failure beyond a certain limit state can be expressed as the convolution of seismic vulnerability and seismic hazard [Aguilar-Meléndez *et al.*, 2019]

$$\lambda_{\mathrm{LS}} = \int_x G(\mathrm{dm}|\mathrm{im})|\lambda_{\mathrm{IM}}(\mathrm{im})|, \tag{17}$$

where λ_{LS} is the annual probability of structure exceeding a certain limit state of failure. When the ground motion intensity parameter is the peak ground acceleration (PGA), the seismic risk can be represented by combining Eq. (13) as follows:

$$\lambda_{\mathrm{LS}} = \int_{\mathrm{PGA}} G(\mathrm{pga})|d\lambda_{\mathrm{PGA}}(\mathrm{pga})|. \tag{18}$$

The seismic probabilistic risk assessment is used to get the probability of some degree of seismic damage in a certain period of time.

2.2. *Seismic loss assessment method*

The losses caused by earthquake disasters mainly include direct loss, indirect loss and casualty. Direct economic loss is the costs associated with the maintenance and replacement of the structure itself due to structural failure. This includes costs related to the damaged load-bearing components, nonload-bearing components and auxiliary structures, as well as the costs of structural repair, restoration and dismantling. Indirect loss refers to the nonphysical economic losses incurred as a result of structural damage, which arise from the inability to use the structure properly. This includes losses such as rental loss, relocation loss, income loss, personal property loss and business inventory loss. However, building structures can potentially cause significant casualties and injuries that cannot be ignored during earthquakes. Therefore, it is crucial to consider casualty as an assessment indicator when assessing the potential disasters caused by earthquakes in structures. It is worth noting that human life is priceless, and the determination of this indicator is solely aimed at establishing unified assessment standards. If it is necessary to include both casualty and seismic losses in the same measurement scale, the casualty can be monetized and defined as the casualty.

$$\mathrm{DV}_i = \mathrm{DV}_i^{\mathrm{BD}} + \mathrm{DV}_i^{\mathrm{RT}} + \mathrm{DV}_i^{\mathrm{REL}} + \mathrm{DV}_i^{Y} + \mathrm{DV}_i^{\mathrm{PP}} + \mathrm{DV}_i^{\mathrm{INV}} + \mathrm{DV}_i^{\mathrm{VDA}}, \tag{19}$$

where DV_i, $\mathrm{DV}_i^{\mathrm{BD}}$, $\mathrm{DV}_i^{\mathrm{RT}}$, $\mathrm{DV}_i^{\mathrm{REL}}$, DV_i^{Y}, $\mathrm{DV}_i^{\mathrm{PP}}$, $\mathrm{DV}_i^{\mathrm{INV}}$, $\mathrm{DV}_i^{\mathrm{VDA}}$ is seismic loss, building loss, rent loss, relocation loss, income loss, personal property loss, business inventory loss and casualty caused by structural damage state in level ith, respectively.

Building loss can be expressed as

$$\mathrm{DV}_i^{\mathrm{BD}} = C_I \times \mathrm{CDF}, \tag{20}$$

where C_I is initial cost of the structure, and CDF is central damage factor of the structure under the ith damage state, as shown in Table 1 [Kassem *et al.*, 2020]. The central damage factor is the proportion of the building loss to the initial cost of

Table 1. Central damage factors for different damage states.

Damage state	Intact	Minor damage	Moderate damage	Severe damaged	Collapse
CDF	0	0.05	0.20	0.80	1

the structure at ith damage state. The values of the central damage factor range from 0–1 ($0 < \mathrm{CDF} < 1$) as shown in Table 1. According to the survey and statistics of relevant experts, Kassem *et al.* [2020] gave the values of the central damage factor in the structure, as shown in Table 1.

Rent loss can be expressed as

$$\mathrm{DV}_i^{\mathrm{RT}} = \mathrm{RT} \times \mathrm{CDF} \times t_i, \tag{21}$$

where RT is the rental loss in ith damage state, which is determined based on rental market prices of the building's location. t_i is the required repair time of ith damage state.

Relocation loss can be expressed as

$$\mathrm{DV}_i^{\mathrm{REL}} = \mathrm{REL} \times \mathrm{CDF} \times t_i, \tag{22}$$

where REL is the relocation loss in ith damage state, which is determined based on social market prices of the building's location.

Income loss can be expressed as

$$\mathrm{DV}_i^{Y} = Y \times \mathrm{CDF} \times t_i, \tag{23}$$

where Y is the income loss for individuals or homeowners due to their inability to work during the reconstruction or repair of C_{I-b} damage state, which is calculated based on the actual income situation.

Personal property loss can be expressed as

$$\mathrm{DV}_i^{\mathrm{pp}} = C_I \times \mathrm{CDF} \times \mathrm{PP}, \tag{24}$$

where PP is the personal property loss in damage state, which is estimated as a percentage of the value of the building, depending on the functional use of the building.

Business inventory loss can be expressed as

$$\mathrm{DV}_i^{\mathrm{INV}} = \mathrm{BI} \times \mathrm{CDF}, \tag{25}$$

where BI is the business inventory loss in ith damage state, which is estimated as a percentage of the sales revenue or production value.

Casualty can be expressed as

$$\mathrm{DV}_i^{\mathrm{VDA}} = \mathrm{NP} \times (\mathrm{MI}_i \times \mathrm{VOL}_i + \mathrm{SI}_i \times \mathrm{VOL}_i + \mathrm{DR}_i \times \mathrm{VOL}_i), \tag{26}$$

where NP is the total population within an individual building, MI_i, SI_i and DR_i are the injury rates of minor injury, serious injury and deaths, respectively, in the ith damage state. Casualty in the ith damage states are shown in Table 2. Casualty rates

Table 2. Casualty rates for different levels of structural damage.

Casualty degree	Intact	Minor damage	Moderate damage	Sever damaged	Collapse
Minor injuries	0	0.00030	0.0030	0.30	0.4
Serious injuries	0	0.00004	0.0004	0.04	0.4
Deaths	0	0.00001	0.0001	0.01	0.2

for different levels of structural damage Agency [2018] are shown in Table 2. VOL_i is the value of human life in the ith damage state.

2.3. *Initial cost assessment method for isolation structures*

The initial cost of isolation structures can be expressed as the sum of the initial cost of the superstructure and the initial cost of the isolation layer

$$C_I = C_{I-s} + C_{I-\mathrm{iso}}, \tag{27}$$

where C_{I-s} is the initial cost of the superstructure; $C_{I-\mathrm{iso}}$ is the initial cost of the isolation layer.

The initial cost of the superstructure is estimated by the estimation index method. The estimation index method calculates the direct project cost of the projects by multiplying the cost per square meter or cubic meter with the construction area or volume. Indirect costs, profits and taxes are then calculated. The formula for direct project cost calculation is

$$\mathrm{DPC} = \mathrm{EPC} \times \mathrm{PA}, \tag{28}$$

where DPC is direct cost, EPC is estimated per square meter (cubic meter) project cost, and PA is construction area (volume).

The calculation formula for the estimated initial project cost of the superstructure is

$$C_{I-s} = \mathrm{DPC} + \mathrm{IC} + P + T, \tag{29}$$

where IC is indirect cost, P is profit, and T is tax.

There are various options for isolation devices, with the commonly used ones being laminated lead-core rubber bearings and dampers. Hence, the initial cost of the isolation layer can be expressed as the sum of the initial cost of laminated lead-core rubber bearings and dampers

$$C_{I-\mathrm{iso}} = C_{I-B} + C_{I-d}, \tag{30}$$

where C_{I-B} is the initial cost of the laminated lead-core rubber bearings; and C_{I-b} is the initial cost of the dampers.

The price of the isolation bearing is related to its volume, as provided by manufacturers, while the cost of the viscous damper is determined not only by its design

displacement under seismic actions but also by its design tonnage. The initial cost of the isolation bearings is

$$C_{I-B} = b_B V_B, \tag{31}$$

where b_B is the price per cubic centimeter of the isolation bearings; V_B is the total volume of the isolation bearings (unit: cm^3). According to the Shanghai Material Institute, the cost of the isolation bearing is approximately 0.3 yuan/cm^3.

The price of viscous dampers is estimated using the least squares method. When the initial cost of a single damper is modeled as a higher-order function of damper tonnage and displacement, the fitting effect is improved.

$$C_{I-d_i} = a_1 + a_2 D_i + a_3 F_i + \sum_{k=0}^{3} (a_{4+3k} D_i^{k+2} + a_{5+3k} D_i^{k+1} F_i + a_{6+3k} D_i^k F_i^2), \tag{32}$$

where C_{I-d_i} is the initial cost of the ith damper (unit: ten thousand yuan); D_i is the maximum displacement of ith damper (unit: m); F_i is the tonnage of ith damper (unit: $\times 10t$); $a_1 \sim a_{14}$ are the fitting coefficients, $a_1 = 4.15$, $a_2 = 6.227$, $a_3 = 0.5777$, $a_4 = 3.354$, $a_5 = 1.309$, $a_6 = -0.07968$, $a_7 = -3.78$, $a_8 = 0.3089$, $a_9 = 1.873$, $a_{10} = -1.572$, $a_{11} = -0.4649$, $a_{12} = 0.4479$, $a_{13} = 1.255$, $a_{14} = -0.02033$ and $a_{15} = -0.9967$ respectively.

The fitted prices are compared with the price provided by the manufacturer, as shown in Table 3. The complex correlation coefficient of the high-order function fitting of the damper is $R^2 = 0.9951$.

3. Performance Levels of the Isolation Structures

Earthquakes can cause varying degrees of structural damage. This paper categorizes the seismic damage states of the isolated structure into five intervals based on four limit states. The four limit states of seismic isolation structures are full operation (LS_1), minor damage (LS_2), life safety (LS_3) and prevent collapse (LS_4). Five damage states are defined as follows: intact (DS_1), slight damage (DS_2), moderate damage (DS_3), severe damage (DS_4) and collapsed (DS_5). The relationship between the limit states and the damage states is shown in Fig. 1.

This paper uses MSD and MDIL as the engineering demand parameters for the isolated superstructure. According to our research group's previous research [Chao *et al.*, 2023], the division standards of MSD and MDIL corresponding to each limit state are obtained, as shown in Table 4.

4. Uncertainty Parameters of the Base-Isolated Structures

In the selection of uncertain parameters, this study focuses on the factors that have the most significant impact on structural strength, stiffness, deformation capacity and energy dissipation characteristics. Based on our research group's previous work [Chao *et al.*, 2023], the uncertain parameters considered in this study include

Table 3. Damper cost fitting.

Tonnage ($\times 10^t$)	Displacement (m)	Actual price ($\times 10^4$ yuan)	Fitted price ($\times 10^4$ yuan)	Absolute error
3	0.5	1.112	0.945	0.15
3	0.1	1.2	0.955	0.20
3	0.15	1.288	1.137	0.12
5	0.05	1.628	1.943	0.19
5	0.1	1.74	2.121	0.22
5	0.15	1.852	2.136	0.15
10	0.05	2.148	1.821	0.15
10	0.1	2.3	2.161	0.06
10	0.15	2.452	2.144	0.13
15	0.05	3.576	4.003	0.12
15	0.1	3.872	4.305	0.11
15	0.15	4.168	4.607	0.11
20	0.05	8.072	7.679	0.05
20	0.1	8.56	7.935	0.07
20	0.15	9.048	8.638	0.05
25	0.05	8.856	9.119	0.03
25	0.1	9.48	9.491	0.00
25	0.15	10.104	10.384	0.03
30	0.05	9.6	9.532	0.01
30	0.1	10.28	10.329	0.00
30	0.15	10.96	10.888	0.01
5	0.1	1.8	2.121	0.18
8	0.1	2.3	2.136	0.07
10	0.1	3	2.161	0.28
15	0.1	3.6	4.305	0.20
18	0.6	25	24.999	0.00

Table 4. Performance design index limits of seismic isolated-reinforced concrete structures.

Limit states	Full operation	Minor damage	Life safety	Prevent collapse
MSD	1/550	1/300	1/150	1/50
MDIL	50%t_r	100% t_r	250% t_r	400% t_r

Note: t_r is the total thickness of the rubber inside the isolation bearing.

compressive strength f_c, elastic modulus E_c, bulk density γ_w of concrete, initial stiffness K_1, the horizontal post-yield stiffness K_d, equivalent stiffness K_h and yield force Q_d. These random variables are assumed to be independent of each other. The probability distribution of random variables of the isolated structure is shown in Table 5.

Regarding the uncertainty of earthquakes, Based on the references, the peak ground acceleration PGA has a great correlation with the peak structural response [Qian and Dong, 2020; Min *et al.*, 2005] and considering that the fortification intensity is the basis of China's seismic fortification, it can be converted into the basic seismic acceleration of design. Therefore, the seismic wave acceleration peak PGA is

Table 5. Statistical characteristics of random variables of isolated structures.

Random variables	Coefficient of variation	Distribution pattern
Compression strength 37.5(MPa)	0.18	Normal distribution
Compression strength 50(MPa)	0.18	Normal distribution
Elasticity modulus 3.0 ($\times 10^4$ N/mm^2)	0.10	Normal distribution
Elasticity modulus 3.25 ($\times 10^4$ N/mm^2)	0.10	Normal distribution
Bulk density 28.35 (kN/m^3)	0.10	Normal distribution
Horizontal post-yield stiffness of isolation bearings	0.15	Normal distribution
Yield force of isolation bearings	0.15	Normal distribution

taken as the ground motion intensity parameter in this study [Hao, 2017], and PGA is considered a random variable. To account for the uncertainty of earthquakes, a large number of seismic waves are selected for seismic response analysis. Studies [Zhou *et al.*, 2021] demonstrated that using more than 60 seismic waves can capture the uncertainty of seismic ground motions.

5. Case Study

5.1. *Project overview*

The life-cycle cost assessment framework proposed is applied to a project of a reinforced concrete frame structure [Chao *et al.*, 2023] as an example. This structure has a basic seismic fortification intensity of 0.3 g. The building has 8 stories and a total area of 9500 m^2. The total height of the building is 29.7 m, the ground floor is 3.9 m high, the 2nd–6th floors are 3.6 m high, the 7th floor is 4.2 m high, and the 8th floor is 3.6 m high. The cross-sectional dimensions of the frame columns are 600 × 600 mm^2, 650 × 650 mm^2 and 700 × 700 mm^2 for the 1st–8th floors. The concrete strength of the 1st–2nd floors is C40, the 3rd–8th floors is C30 and the floor main beam section size is 350 × 620 mm^2 and 350 × 820 mm^2, the secondary beam section size is 250 × 550 mm^2 and 250 × 500 mm^2. The architectural structure plan is shown in Fig. 4. To reduce the seismic effects of the superstructure, a seismic isolation layer was installed at the top of the columns on the first floor. The seismic fortification intensity of the superstructure was designed to be reduced by 0.15 g after apply base-isolated. The lead rubber bearings were selected as the isolation devices due to their good damping effects provided by the lead core. The plan layout of seismic isolation bearings is shown in Fig. 5. The mechanical properties of the isolation bearings are shown in Table 6. A total of 43 isolation bearings were installed, and the total horizontal stiffness of isolation bearings is 84 kN/mm.

5.2. *Comparison of seismic vulnerability analysis on base-isolated and nonisolated structures*

The random variables of the nonisolated structure are the same as the superstructure of the base-isolated structure, including the modulus of elasticity of concrete E_c,

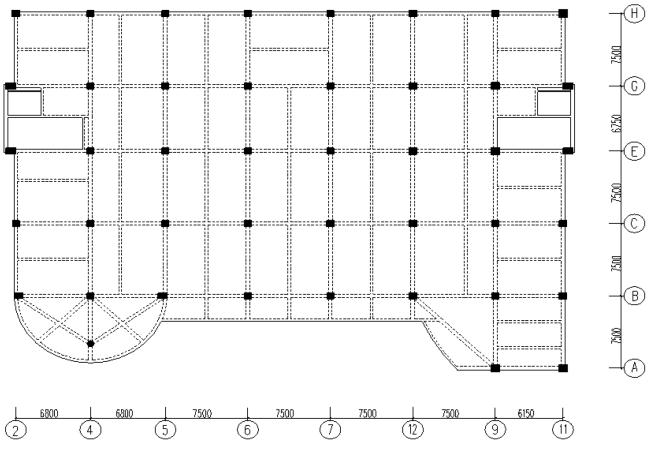

Fig. 4. Architectural structure plan.

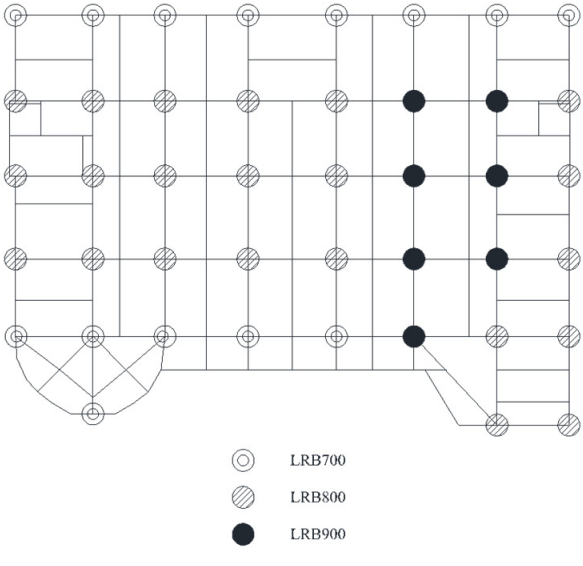

Fig. 5. Seismic isolation bearings plan layout.

structural capacity γ_w and PGA. MSD is selected as the engineering demand parameter for the nonisolated structure. The ground motions used to conduct nonlinear time-history analysis are also the same as those applied to the base-isolated structure.

Once the structural response surface functions are established, the seismic vulnerability curves of the nonisolated structure are plotted and compared with those of the isolated structure, as shown in Fig. 6. The exceeding probabilities of the non-isolated structure under minor, moderate and major earthquakes are listed and compared with the isolated structure's probabilities, as shown in Table 7.

Table 6. Mechanical properties of lead rubber bearings.

Product model	Datum pressure (MPa)	Long-term load kN/mm	Vertical stiffness Kv kN/mm	Initial stiffness K1 kN/mm	Post-yield stiffness Kd kN/mm	Equivalent stiffness Kh kN/mm	Yield strength Qd (kN)	Damping ratio Heq (%)
LRB700	15	5603	3157	14.213	1.093	1.643	76	20.4
LRB800	15	7275	3671	16.447	1.265	2.052	123	23.1
LRB900	15	9202	4260	18.511	1.424	2.337	160	23.5

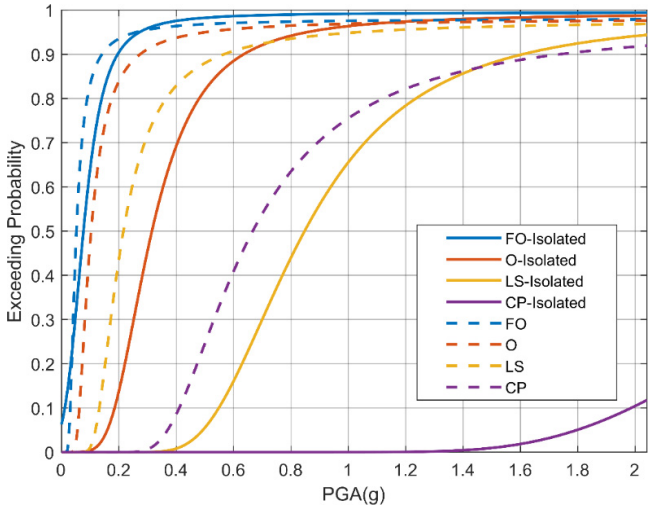

Fig. 6. Seismic vulnerability curves of the base-isolated and the nonisolated structures.

Figure 6 and Table 7 show that the implementation of seismic isolation measures can significantly reduce the failure probability of the structure under different seismic intensity levels. The exceeding probability of the structure after seismic isolation decreases more under moderate and major earthquakes, thanks to the effective seismic mitigation effects of isolation bearings. Under a moderate earthquake, the exceeding probability of the minor damage limit state decreases from 91% to 47%, while the exceeding probability of the life safety limit state decreases from 73% to 0%.

Table 7. Exceeding probability of the base-isolated and nonisolated structures.

Exceeding probability		P_{LS_1}	P_{LS_2}	P_{LS_3}	P_{LS_4}
Nonisolated structure	Minor earthquake	0.86	0.57	0.03	0.00
	Moderate earthquake	0.96	0.91	0.73	0.01
	Major earthquake	0.97	0.95	0.89	0.28
Base-isolated structure	Minor earthquake	0.70	0.01	0.00	0.00
	Moderate earthquake	0.96	0.47	0.00	0.00
	Major earthquake	0.98	0.84	0.07	0.00

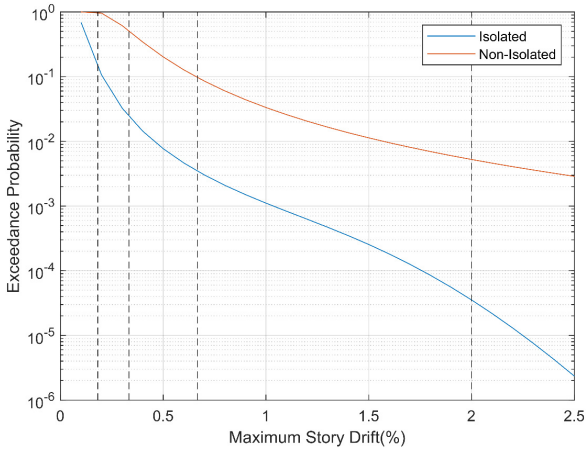

Fig. 7. 50-year exceeding probability curves of the base-isolated and nonisolated structures.

5.3. *Comparison of seismic probabilistic risk assessment on base-isolated and nonisolated structures*

Based on Eq. (17), the annual probability of structural damage state exceeding a certain limit state can be calculated by combining seismic hazard analysis and seismic vulnerability analysis. The seismic risk of the base-isolated structure during the 50-year design period can be deduced from the annual seismic risk, as shown in Eq. (33)

$$\lambda_{\mathrm{LS}}^{50} = 1 - (1 - \lambda_{\mathrm{LS}})^{50} \tag{33}$$

where $\lambda_{\mathrm{LS}}^{50}$ indicates the exceeding probability that the structural damage state is beyond a certain limit state in a 50-year design period. Fig. 7 shows the 50-year seismic risk curve of the base-isolated and nonisolated structure. Table 8 compares the 50-year exceeding probabilities of the base-isolated and nonisolated structures for the four performance levels, it can be observed that the exceeding probability of fully operational, minor damage, life safety and prevent collapse limit states of the seismic isolation system are 19.76%, 3.89%, 0.51% and 0.05%, respectively. During the 50-year design period, the seismic isolation structure can ensure not only the structural life safety but also the structural function integrity.

Figure 7 and Table 8 show that the seismic risk of the structure is greatly reduced after implementing isolation measures. The nonisolated structure has a 50.72%

Table 8. 50-year exceeding probability of the base-isolated and nonisolated structures (%).

Performance 50-year exceeding probability	Fully operational	Minor damage	Life safety	Prevent collapse
Base-isolated structure	19.76	3.89	0.51	0.05
Nonisolated structure	98.70	50.72	9.72	0.53

Table 9. Recovery to 100 % of the time when the building is in a different state of damage (day).

	Intact	Minor damage	Moderate damage	Severe damaged	Collapse
t_i	0	56	156.8	613.2	723.4

probability of exceeding the limit state of minor damage and a 9.72% probability of exceeding the life safety limit state during the 50-year design period. In contrast, the seismic isolation structure not only ensures the life safety of the structure but also maintains the integrity of the structural function over the 50-year design period.

5.4. *Comparison of seismic loss on base-isolated and nonisolated structures*

According to the China Statistical Yearbook [2022], the local relocation loss was $9/m^2/day$, income loss was 139.65×10^4 yuan and the total population in the building is 665 people. According to FEMA 227, the percentage of personal property loss in this structure was 80%, and the time taken to recover to 100% under different failure states is shown in Table 9. The values of human life VOL is according to the Work Injury Insurance Regulations, as shown in Table 10.

Based on the seismic loss assessment method and Eq. (7), seismic loss of the base-isolated and nonisolated structures over a 50-year design period can be calculated, as shown in Table 11. Table 11 shows that the maximum proportion (66%) of seismic loss is attributed to income loss, resulting from the high income of the hospital The second largest proportion (17%) of seismic loss is building loss, attributed to the high initial construction cost. The smallest proportion (0.2%) of seismic loss is casualty, resulting from the low probability of seismic damage in the isolated structure. The assessment of business inventory loss applies to commercial buildings, but since this building is a hospital, business inventory loss is not applicable. Furthermore, the superstructure remains functional after implementing reinforcement measures, which excludes relocation loss as well.

5.5. *Comparison of life-cycle cost on base-isolated and nonisolated structures*

Table 12 lists the life-cycle cost of the isolated and nonisolated structures over the 50-year design period. Table 12 shows that the isolated structure incurs a relatively high initial cost compared to the nonisolated structure, mainly due to its smaller seismic

Table 10. The value of human life VOL in different casualty states ($\times 10^4$ yuan).

Casualty degree	Minor injuries	Serious injuries	Deaths
VOL_i	3.01	11.93	54.80

Table 11. Seismic loss of the base-isolated and nonisolated structures over a 50-year design period ($\times 10^4$ yuan).

Damage state		Intact	Minor damage	Moderate damage	Severe damaged	Collapse	Ratio to seismic loss
Building loss	Base-isolated	0	21	14	0	0	17%
	Nonisolated	0	79	271	238	33	6%
Rent loss	Base-isolated	0	3	5	0	0	4%
	Nonisolated	0	11	110	377	62	5%
Income loss	Base-isolated	0	47	88	0	0	66%
	Nonisolated	0	188	1796	6166	1010	83%
Personal property loss	Base-isolated	0	17	11	0	0	14%
	Nonisolated	0	64	217	191	26	4%
Casualty	Base-isolated	0	0.2	0.3	0	0	0.2%
	Nonisolated	0	0.6	5	117	113	2%
Seismic loss	Base-isolated	0	87	118	0	0	–
	Nonisolated	0	343	2400	7089	1245	–
	Base-isolated/Nonisolated	–	25%	5%	0%	0%	–

Table 12. Life-cycle costs of the isolated and nonisolated structures over 50-year design period ($\times 10^4$ yuan).

Cost	Initial cost	Seismic loss	Life-cycle cost	Initial cost/life-cycle cost
Base-isolated	3438	205	7869	43.69%
Nonisolated	3311	11077	24275	13.64%
Base-isolated/Nonisolated	104%	1.85%	32.42%	–

loss proportion. On the other hand, the nonisolated structure experiences a relatively large seismic loss, leading to a smaller proportion of the initial cost in its life-cycle cost. Additionally, even though the initial cost of the isolated structure exceeds that of the nonisolated structure, its seismic loss and life-cycle cost are only 1.85% and 32.42% of those of the nonisolated structure, respectively. This indicates a significant reduction in seismic loss and life-cycle cost after implementing isolation measures.

6. Conclusions

This paper presented a performance-based assessment method to assess the seismic losses and life-cycle costs of base-isolated structures, offering assessment tools for project decision-making. Firstly, we adopted a comprehensive seismic probabilistic risk assessment framework that integrates seismic hazard analysis and seismic vulnerability analysis to calculate the probabilities for each damage state. In the seismic vulnerability analysis, we introduced the dual response surface method to improve computational efficiency while ensuring accuracy. Secondly, formulas for calculating rental losses, relocation losses, income losses, personal property losses, business inventory losses and casualties are provided, quantifying the cost of casualties and integrating casualties into a unified assessment system. These losses are all related to

the damage state of the building. Lastly, we defined the initial cost of the isolation structure as the sum of the superstructure and isolation layer costs. The initial cost of the superstructure was estimated using the cost index method, while the initial cost of the isolation layer was determined by summing the costs of isolation bearings and dampers. The cost of isolation bearings was determined by their volume, while the cost of dampers was calculated using their stroke and tonnage. By integrating the initial cost with the seismic loss assessment and considering the annual discount rate, we could evaluate the life-cycle cost of the base-isolated structures. Finally, taking an 8-story-reinforced concrete structure as an example, the seismic hazard, seismic vulnerability and seismic risk are analyzed, and the initial cost, seismic losses and life-cycle cost of the structure are assessed. By comparing the seismic losses and life-cycle costs of the two types of structures, we derive specific conclusions:

The proportion of initial cost and seismic loss to the life-cycle cost of isolated and nonisolated structures is calculated. The initial cost and the seismic loss of the isolated structure account for 43.69% and 2.61% of the life-cycle cost, respectively. Among them, the building loss, rental loss, income loss, personal property loss and casualty of the isolation structure account for 0.44%, 0.10%, 1.72%, 0.36% and 0.01% of the life-cycle cost, respectively. The initial cost and the seismic loss of the non-isolated structure account for 13.64% and 45.63% of the life-cycle cost, respectively. Among them, the building loss, rental loss, income loss, personal property loss and casualty of the nonisolated structure account for 2.56%, 2.31%, 37.73%, 2.05% and 0.97% of the life-cycle cost, respectively. In the life-cycle cost of isolated and non-isolated structures, the proportion of income loss is the maximum, resulting from the high income of the hospital, and the proportion of casualties is the minimum, which is due to the good performance of reinforced concrete structures.

The implementation of isolation devices led to a 3.69% increase in the initial cost, the seismic loss of the isolated structure is 1.85% of that of the nonisolated structure, the life-cycle cost of the isolated structure is 32.42% of that of the nonisolated structure. Among them, isolated structure compared with the nonisolated structure, the building loss, the rental loss, the income loss, the personal property loss and the casualties were reduced by 94.36%, 98.57%, 98.53%, 94.38% and 99.79% respectively. Although the adoption of seismic isolation measures will increase the initial cost, it can greatly reduce the seismic loss and the life-cycle cost of the structure. The implementation of seismic isolation measures can significantly reduce the failure probability of the structure under different seismic intensity levels. The exceeding probability of the structure after seismic isolation decreases more under moderate and major earthquakes, thanks to the effective seismic mitigation effects of isolation bearings.

The life-cycle cost assessment method proposed in this paper is easy to implement and has yielded positive assessment results. The proposed base-isolation technique in this paper effectively reduces casualty and economic losses caused by earthquakes. The life-cycle cost assessment also predicted the social losses due to earthquakes, thereby facilitating decision-making analysis by relevant departments. This paper

has conducted seismic vulnerability analysis, seismic probability risk analysis and seismic loss assessment for isolated structures, leading to the conclusions mentioned above. However, there was still room for improvement and further research in this area, and the following aspects warranted additional investigation and discussion:

(1) This paper used PGA as a random variable to represent the seismic vulnerability and risk of the isolated structures. Further investigation of other ground motion intensity parameters, such as spectral acceleration Sa, peak ground velocity PGV, peak ground displacement PGD, etc., is warranted.
(2) The dual response surface method proposed in this paper is limited to situations involving fewer than 5 random variables, otherwise the calculation workload is too large, and a more efficient seismic vulnerability assessment method can be studied.

Acknowledgments

This study was funded by the independent projects for the State Key Laboratory of Mechanical Behavior and System Safety of Traffic Engineering Structures [grant Nos. ZZ2021-03]; the Natural Science Foundation of Hebei Province (CN) [grant No. E202210095, E2024210049]; S&T Program of Hebei (CN) [grant No. 21375407D]; Science and Technology Research and Development Program of CHINA RAILWAY [grant No. P2022G013]; the Project of Central Guiding Local Science and Technology Development Funds (Fundamental Research Project) [Grant No. 216Z5402G].

ORCID

Hao Wang https://orcid.org/0000-0002-7463-1433
Xiaoxia Guo https://orcid.org/0009-0000-5612-6823
Chao Luo https://orcid.org/0000-0003-3166-7644
Jun Zhao https://orcid.org/0009-0000-2521-8450
Huaiping Feng https://orcid.org/0000-0003-2435-1027

References

Aguilar-Meléndez, A., Pujades, L. G., Barbat, A. H., Ordaz, M. G., de la Puente, J., Lantada, N. and Rodríguez-Lozoya, H. E. [2019] "A probabilistic approach for seismic risk assessment based on vulnerability functions. Application to Barcelona," *Bull. Earthq. Eng.* **17**, 1863–1890, doi: 10.1007/s10518-018-0516-4.

Altunişik, A. C., Arslan, M. E., Kahya, V., Aslan, B., Sezdirmez, T., Dok, G., Kirtel, O., öztürk, H., Sunca, F., Baltaci, A., Emiroğlu, M., Günaydin, M., Adanur, S., Atmaca, B., Akgül, T., Demir, A., Tatar, T., Aykanat, B., Haciefendioğlu, K., Saribiyik, A., Yurdakul, M., Akbulut, Y. E., Okur, F. Y., _en, F., Genç, A. F., Başağa, H. B., Demirkaya, E., Güleş, O. and Nas, M. [2023] "Field observations and damage evaluation in reinforced concrete buildings after the February 6th, 2023, kahramanmaraş–türkiye earthquakes," *J. Earthq. Tsunami* **17**, 2350024-1–2350024-54 (54 pages), doi: 10.1142/S1793431123500240.

Altunişik, A. C., Atmaca, B., Kartal, M. E., Günaydin, M., Demir, S. and Uluşan, A. [2021] "Assessment of structural damage following the October 30, 2020 Aegean sea earthquake and tsunami," *J. Earthq. Tsunami* **15**, doi: 10.1142/S1793431121500299.

Arash Rayegani, G. N. [2022] "Seismic collapse probability and life cycle cost assessment of isolated structures subjected to pounding with smart hybrid isolation system using a modi ed fuzzy based controller," *Structures* **44**, 30–41, doi: 10.21203/rs.3.rs-1239670/v1.

Astorga, A., Guéguen, P., Ghimire, S. and Kashima, T. [2020] "Nde1.0: A new database of earthquake data recordings from buildings for engineering applications," *Bull. Earthq. Eng.* **18**, 1321–1344, doi: 10.1007/s10518-019-00746-6.

Aykanat, B., Ertürk, E., Altunışık, A. C. and Aslan, M. E. [2023] "Field investigation on reinforced concrete and masonry buildings damages after November 23, 2022 gölyaka (düzce) earthquake," *J. Earthq. Tsunami* **17**, doi: 10.1142/S1793431123500100.

Bashir, A. and Basu, D. [2018] "Revisiting probabilistic seismic hazard analysis of Gujarat: An assessment of Indian design spectra," *Nat. Hazards* **91**, 1127–1164, doi: 10.1007/s11069-018-3171-9.

Chao, L., Hao, W., Xiaoxia, G., Feiyu, W., Kexin, T. and Huaiping, F. [2023] "Seismic fragility analysis of base-isolated structures based on response surface method," *ASCE ASME J. Risk Uncertain. Eng. Syst. Part A: Civ. Eng.* **9**, 05023002-1–05023002-12 (12 pages), doi: 10.1061_AJRUA6.RUENG-1020.

Cornell, A. [1968] "Engineering seismic risk analysis," *Bull. Seismol. Soc. Am.* **58**(5), 1583–1606.

Council, A. T. [2018]. Seismic Performance Assessment of Buildings Volume 1 – Methodology.

Demir, S., Günaydin, M., Atmaca, B., Altunişik, A. C., Hüsem, M., Adanur, S., Angin, Z. and Ateş, S. [2021] "Performance evaluation of reinforced concrete buildings during the sivrice-elazığ earthquake (mw = 6.8, January 24, 2020) in accordance with Turkish earthquake code," *J. Earthq. Tsunami* **15**, doi: 10.1142/S1793431121500184.

Dolce, M., Prota, A., Borzi, B., Da Porto, F., Lagomarsino, S., Magenes, G., Moroni, C., Penna, A., Polese, M., Speranza, E., Verderame, G. M. and Zuccaro, G. [2021] "Seismic risk assessment of residential buildings in italy," *Bull. Earthq. Eng.* **19**, 2999–3032, doi: 10.1007/s10518-020-01009-5.

Du, K., Bai, W. and Bai, J. [2021] "Comparative seismic performance assessment of reinforced concrete frame structures with and without structural enhancements using the fema p-58 methodology," *ASCE-ASME J. Risk Uncertainty Eng. Syst., Part A: Civ. Eng.*, 1–18, doi: 10.1061/AJRUA6.0001173.

Galvis, F. A., Miranda, E., Heresi, P., Dávalos, H. and Ruiz-García, J. [2020]. Overview of collapsed buildings in mexico city after the 19 september 2017 (mw 7.1) earthquake. *Earthq. Spectra* **36**, 83–109. doi: 10.1177/8755293020936694.

Gerstenberger, M. C., Marzocchi, W., Allen, T., Pagani, M., Adams, J., Danciu, L., Field, E. H., Fujiwara, H., Luco, N., Ma, K. F., Meletti, C. and Petersen, M. D. [2020] "Probabilistic seismic hazard analysis at regional and national scales: State of the art and future challenges," *Rev. Geophys.* **58**, doi: 10.1029/2019RG000653.

Gil-Oulbé, M., Al-Shaibani, F. A. N. A. and Lina, A. S. [2020] "Performance-based seismic design for buildings," *Struct. Mech. Eng. Constr. Build.* **16**, 161–166, doi: 10.22363/1815-5235-2020-16-2-161-166.

Hao, W. [2017] "Seismic vulnerability analysis of base isolation structures and seismic risk assessment." PhD program, Tongji University.

Kassem, M. M., Mohamed Nazri, F. and Noroozinejad Farsangi, E. [2020] "The seismic vulnerability assessment methodologies: A state-of-the-art review," *Ain Shams Eng. J.* **11**, 849–864, doi: 10.1016/j.asej.2020.04.001.

Katsamakas, A. A., Chollet, M., Eyyi, S. and Vassiliou, M. F. [2021] "Feasibility study on reusing tennis balls as seismic isolation bearings," *Front. Built Environ.* **7**, doi: 10.3389/fbuil.2021.768303.

Kharde, S. H. and Soni, D. P. [2022] "Seismic response mitigation of extra-large lng storage tanks," *J. Earthq. Tsunami* **16**, 2250014, doi: 10.1142/S1793431122500142.

Lee, G., Lee, G., Seokho Chi, M. A., and Oh, S. [2023] "Automatic classification of construction work codes in bill of quantities of national roadway based on text analysis," *J. Constr. Eng. Manage* **2**, 04022163-1–04022163-13 (13 pages), doi: 10.1061/JCEMD4.COENG-12730.

Li, T. Z. and Yang, X. L. [2019] "An efficient uniform design for kriging-based response surface method and its application," *Comput. Geotech.* **109**, 12–22, doi: 12-22.10.1016/j.compgeo.2019.01.009.

Liu, J., Song, D., Li, Q., Yang, J., Hu, Y., Fang, F. and Hoon Joo, Y. [2023] "Life cycle cost modelling and economic analysis of wind power: A state of art review," *Energy Convers. Manag.* **277**, 116628, doi: 10.1016/j.enconman.2022.116628.

Min, H., Li-Li, X. and Long-Jun, X. [2005] "Some considerations on the physical measure of seismic intensity," *Acta Seismol. Sin.* **18**, 245–250.

Norio, O., Tao, Y., Kajitani, Y., Peijun, S. and Tatano, H. [2011] "The 2011 eastern japan great earthquake disaster; Overview and comments," *Int. J. Disaster Risk Sci.* **2**, 34–42, doi: 10.1007/s13753-011-0004-9.

Nouri, A., Asadi, P. and Taheriyoun, M. [2022] "Life-cycle cost analysis of seismic designed rc frames including environmental and social costs," *J. Earthq. Eng.* **26**, 5958–5977, doi: 10.1080/13632469.2021.1911877.

O'Reilly, G. J. and Calvi, G. M. [2019] "Conceptual seismic design in performance-based earthquake engineering," *Earthq. Eng. Struct. Dyn.* **48**, 389–411, doi: 10.1002/eqe.3141.

Qian, J. and Dong, Y. [2020] "Multi-criteria decision making for seismic intensity measure selection considering uncertainty," *Earthq. Eng. Struct. Dyn.* **49**, 1095–1114, doi: 10.1002/eqe.3280.

Sevim, B., Ayvaz, Y., Akbulut, S., Aydıner, M. F., Uzun, S. and Ari, A. [2024] Seismic performance and damage evaluation of reinforced concrete structures based on field investigation made after February 6, 2023, kahramanmaraş earthquakes," *J. Earthq. Tsunami* **18**, doi: 10.1142/S179343112350032X.

Wang, G., Ba, F., Ma, X., Zhao, J. and Yue, Y. [2021] "Research on seismic reduction and isolation measures for urban underground station structure," *J. Earthq. Tsunami* **15**, 2150012-1–2150012-21 (21 pages), doi: 10.1142/S1793431121500123.

Wang, N. and Huang, X. [2021] "Global damage model for the seismic reliability analysis of a base-isolated structure," *Structures* **34**, 4892–4907, doi: 10.1016/j.istruc.2021.10.059.

Zhou, Y., Zhang, Y., Pang, R. and Xu, B. [2021] "Seismic fragility analysis of high concrete faced rockfill dams based on plastic failure with support vector machine," *Soil Dyn. Earthq. Eng.* **144**, 106587, doi: 10.1016/j.soildyn.2021.106587.